10-2013

Structure-dependent Inhibition of the ETS-Family Transcription Factor PU.1 by Novel Heterocyclic Diamidines

Manoj Munde
Georgia State University, mmunde@mail.jnu.ac.in

Shuo Wang
shuow22@gmail.com

Arvind Kumar
Georgia State University, akumar@gsu.edu

Chad E. Stephens
Georgia State University, cstephe7@aug.edu

Abdelbasset A. Farahat
Georgia State University, afarahat@gsu.edu

See next page for additional authors

Published online 23 October 2013 *Nucleic Acids Research, 2014, Vol. 42, No. 2* ***1379–1390***
doi:10.1093/nar/gkt955

Structure-dependent inhibition of the ETS-family transcription factor PU.1 by novel heterocyclic diamidines

Manoj Munde[1], Shuo Wang[1], Arvind Kumar[1], Chad E. Stephens[1], Abdelbasset A. Farahat[1], David W. Boykin[1], W. David Wilson[1] and Gregory M. K. Poon[2,*]

[1]Department of Chemistry, Georgia State University, Atlanta, GA 30303, USA and [2]Department of Pharmaceutical Sciences, Washington State University, Pullman, WA 99164-6534, USA

Received July 11, 2013; Revised September 25, 2013; Accepted September 27, 2013

ABSTRACT

ETS transcription factors mediate a wide array of cellular functions and are attractive targets for pharmacological control of gene regulation. We report the inhibition of the ETS-family member PU.1 with a panel of novel heterocyclic diamidines. These diamidines are derivatives of furamidine (DB75) in which the central furan has been replaced with selenophene and/or one or both of the bridging phenyl has been replaced with benzimidazole. Like all ETS proteins, PU.1 binds sequence specifically to 10-bp sites by inserting a recognition helix into the major groove of a 5′-GGAA-3′ consensus, accompanied by contacts with the flanking minor groove. We showed that diamidines target the minor groove of AT-rich sequences on one or both sides of the consensus and disrupt PU.1 binding. Although all of the diamidines bind to one or both of the expected sequences within the binding site, considerable heterogeneity exists in terms of stoichiometry, site–site interactions and induced DNA conformation. We also showed that these compounds accumulate in live cell nuclei and inhibit PU.1-dependent gene transactivation. This study demonstrates that heterocyclic diamidines are capable of inhibiting PU.1 by targeting the flanking sequences and supports future efforts to develop agents for inhibiting specific members of the ETS family.

INTRODUCTION

Transcription factors (TFs) are central to many cellular process and account for 5–10% of genes in eukaryotes (1). The central role of transcriptional regulation in numerous cellular pathways provides strong rationale for TFs as attractive targets for pharmacologic control (2–4). Specifically, small-molecule inhibitors that block TFs from binding to regulatory sites can lead to novel therapeutics for a wide range of human diseases. They also complement macromolecular approaches for inhibiting gene expression, such as anti-sense oligonucleotides, RNAi and stapled peptides, which suffer from weak metabolic stability and poor cell uptake properties *in vivo* (5,6). Although the design of small molecules that specifically modulate TFs has proved challenging, recent activities have witnessed significant progress. For example, sequence-specific polyamides have been shown to effectively block some TFs from binding to their target DNA sites (7–11). Heterocyclic diamidines have also shown excellent inhibition of several TF-DNA complexes, with the potential for development as anticancer therapeutics (12,13).

The ETS family of TFs controls a wide array of physiologic processes in many tissues (14–17) and is involved in a large number of diseases, particularly cancers, in which it causes aberrant gene expression (18–21). In addition, the signaling pathways of several autoimmune diseases depend on receptors (e.g. IL-2Rγ, IL-7Rα, Toll-like receptors), whose expression is regulated by specific ETS members such as PU.1 (22–26). As sequence-specific binding is an obligate step in ETS-mediated gene activation, inhibiting the appropriate ETS–DNA complex with

*To whom correspondence should be addressed. Tel: +509 335 8341; Fax: +509 335 5902; Email: gpoon@wsu.edu
Present addresses:
Chad E. Stephens, Department of Chemistry and Physics, Georgia Regents University, 2500 Walton Way, Augusta, GA 30904, USA.
Abdelbasset A. Farahat, Department of Pharmaceutical Organic Chemistry, Faculty of Pharmacy, Mansoura University, Mansoura 35516, Egypt.

small molecules offers significant potential to impact therapy for a broad range of diseases. All ETS proteins share a conserved DNA binding domain that recognizes sites harboring a 5′-GGAA/T-3′ consensus. The protein inserts α-helix contacts into the major groove of the core sequence, whereas loops interact with flanking bases via backbone contacts at the minor groove (14). These flanking sequences are often conserved for specific ETS members, and compounds with high affinity for binding in the DNA minor groove may be developed as effective allosteric inhibitors of ETS–DNA complexes.

In the present study, we report the modulation of PU.1 by small molecules *in vitro* and in live cells. Recent thermodynamic studies have advanced our molecular understanding of sequence recognition by PU.1 (27–29). PU.1 belongs to a restricted class of ETS proteins (class III) that is strongly selective for AT-rich flanking sequences, a feature that is distinct from other ETS classes (30). We are interested in the potential of AT-targeting heterocyclic diamidines to inhibit the PU.1-DNA complex. As PU.1 and compound are not directly competing for the same DNA binding site, inhibition of major groove-binding TFs by minor-groove binding small molecules is a complex task (9,31).

Here we demonstrate, using the λB motif of the Ig2–4 enhancer (32), a high-affinity PU.1 binding site with AT-rich tracks flanking both sides of the ETS consensus, how gene-specific compound inhibition can be achieved by targeting sequences that flank the conserved GGAA site. We have recently optimized a biosensor-surface plasmon resonance (SPR)-based screen to identify compounds that target the PU.1-λB complex (27). Together with additional characterization by electrophoretic mobility shift and DNA footprinting, the data reveal that, although all compounds examined bind to the same expected motif(s) within the λB site, significant heterogeneity exists in terms of stoichiometry, site–site interactions and induced DNA conformation. The compounds also exhibit structure- and group-dependent differences in PU.1 inhibition and nuclear localization in live unfixed cells without detectable toxicity. These results establish the potential of heterocyclic diamidines as viable therapeutics for PU.1 and other ETS family of TFs.

MATERIALS AND METHODS

DNA, protein and compounds

Synthetic DNA was obtained from Integrated DNA Technologies (Coralville, IA, USA). The ETS domain of murine PU.1 (residues 167–272) was overexpressed in *Escherichia coli* and purified as described (28). The compounds of Figure 1A were synthesized as previously described and new compound synthesis is presented in the Supplementary Methods. Their purity was verified by NMR and elemental analysis. Concentrated stock solutions (1 mM) were prepared in water.

Biosensor-SPR assays for binding affinity and PU.1-DNA complex inhibition

SPR measurements were performed with a four-channel Biacore T200 optical biosensor system (GE Healthcare). A 5′-biotin labeled hairpin DNA sample (Figure 1B) was immobilized onto CM4 chips as previously described (27). Detailed description of direct binding SPR experiment and data analysis may be found in the Supplementary Methods.

For compound inhibition studies, protein was injected at a constant concentration of 100 nM onto the surface to saturate DNA binding sites. Graded concentrations of compound were then added to the protein solution. The change in protein signal was plotted against compound concentration with the midpoint of the transition taken as IC_{50} (concentration required to achieve 50% protein inhibition) value. Detailed descriptions of complementary electrophoretic gel mobility shift assays are provided in the Supplementary Methods.

DNA footprinting

Using the recombinant pUC19 plasmid described earlier in text, internal primers were used to generate ∼100-bp singly 5′-radiolabeled λB fragments by PCR. After purification by agarose gel extraction, the λB fragment was mixed with a saturating concentration of compound in the same buffer as in gel mobility shift experiments. At equilibrium, samples were digested with DNase I or chemically generated hydroxyl radicals (•OH) and subsequently purified as previously described (28), along with selected chemical sequencing reactions for base identification. After denaturing electrophoresis, the gel was dried and digitized by phosphorimagery at a resolution of 200 μm.

Reporter assay for PU.1 activity in live cells

An expression plasmid encoding full-length PU.1 was cloned between the NheI/BamHI sites of pcDNA3.1 (+). Separately, the CMV promoter of a commercial enhanced green fluorescent protein (EGFP) reporter plasmid (pEGFPLuc; Clontech) was replaced with a synthetic enhancer element consisting of five tandem repeats of the λB site, spaced one helical-turn apart and followed by a minimal TATA-box promoter (33). The PU.1 expression and EGFP reporter plasmids are designated pcDNA-FL-PU.1 and pλB × 5-EGFP, respectively. HEK293 cells, cultured in RPMI 1680 medium containing 10% fetal bovine serum under 5% CO_2 at 37°C, were seeded in 24-well plates (20×10^4 cells) and transfected with 500 ng of pcDNA-FL-PU.1 after 24 h (JetPRIME, Polyplus-transfection, Illkirch, France). The cells were retransfected 24 h later with 500 ng of the pλB × 5-EGFP plasmid with or without compounds. Cellular fluorescence was quantified by flow cytometry (excitation/emission = 488/510 nm). Counts were collected to >20 000 per sample, corresponding to a CV of <5% for a 2% event frequency and gated against untransfected controls to eliminate background. Separately, cell viability was evaluated by the metabolic reduction of resazurin to fluorescent resorufin (530/590 nm) using a commercial reagent (Cell-Titer Blue, Promega) after incubation with the compounds for 24 h.

Fluorescence microscopy of cellular uptake of the heterocyclic dications

HEK293 cells were seeded on chambered glass slides (Lab-Tek; Corning), previously coated with poly-L-lysine,

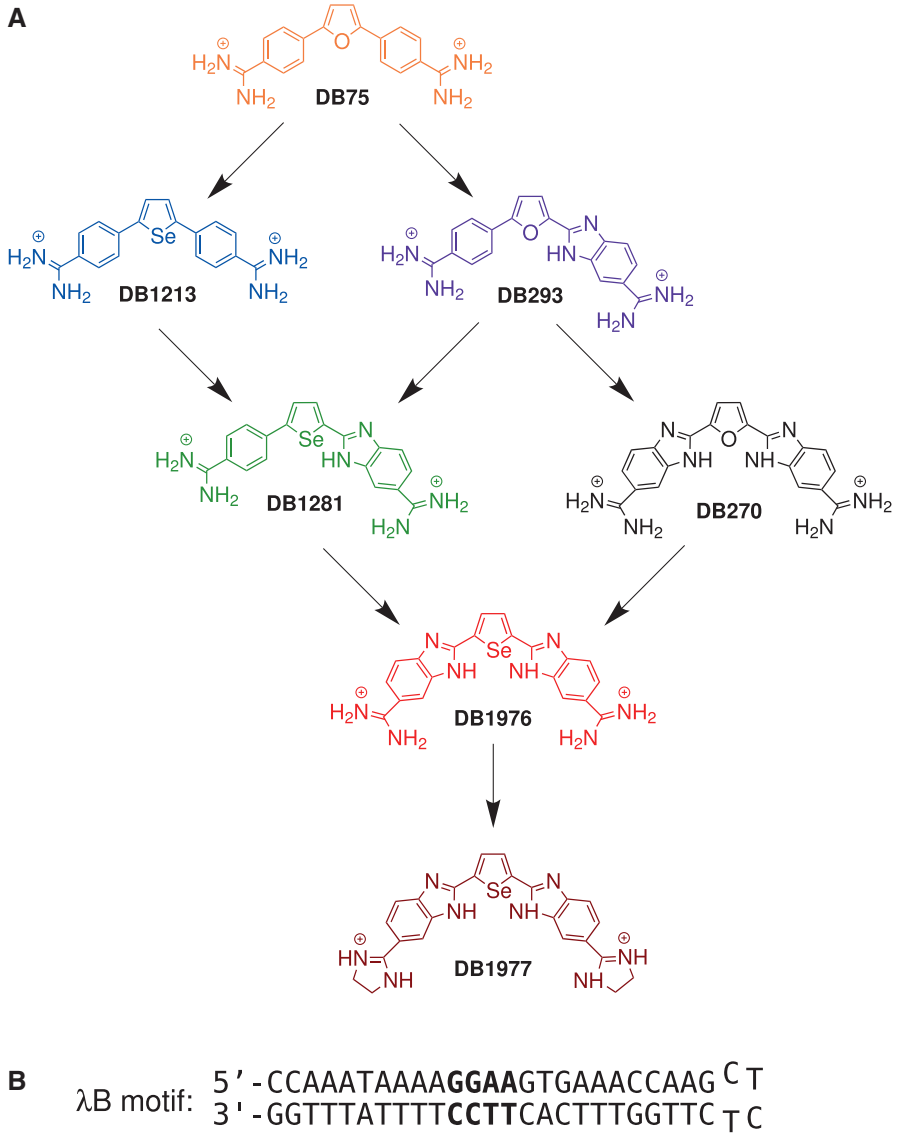

Figure 1. Heterocyclic diamidines and DNA target site used in this study. (**A**) Compounds are colored to aid visualization of the succeeding figures. (**B**) The high-affinity λB site hairpin used in SPR experiments. The ETS consensus sequence (5′-GGAA-3′) is in bold.

with 10 μM compounds for 24 h. Before microscopic examination, doxorubicin (DOX) was added at 2 μg/ml and incubated for 30 min. Medium was removed and cells were washed twice with PBS. The compounds and DOX were visualized on a Zeiss Axio Observer.Z1 fluorescence microscope with a 365/445 nm and 570/630 nm filter set (Chroma), respectively. Imagery was acquired with a Hamamatsu ORCA-AG CCD camera. Colocalization statistics were performed using Axiovision software (Release 4.8.0.0; Zeiss) as described (34,35).

RESULTS

Heterocyclic diamidines target the minor groove of the λB site, a high-affinity cognate sequence for PU.1

Starting with DB75 (furamidine), a well-characterized paradigm from the heterocyclic diamidine family, we selected a panel of seven related compounds with a variety of structures and functional groups (Figure 1A) to determine whether they can inhibit binding of PU.1 to the λB site. The compounds were first screened for binding to the λB site by SPR analysis (Figure 2A and Table 1). The parent DB75 bound the λB site relatively weakly (K_D = 0.53 μM), and single modifications in terms of substitution of the furan by selenophene (DB1213) or a monobenzimidazole derivative (DB293) did not significantly improve affinity. DB293 did exhibit a sigmoidal binding curve, indicative of positively cooperative binding as a stacked dimer to the 5′-AAATAAA-3′ sequence at the 5′ side of the λB site (Supplementary Figure SD1), as previously observed with other sequences for this compound (36). When the two modifications in DB1213 and DB293 were combined (DB1281), affinity was improved by ∼10-fold. DB270 is the bisbenzimidazole-furan analog of DB293 and it also binds significantly more tightly than DB293 and similarly

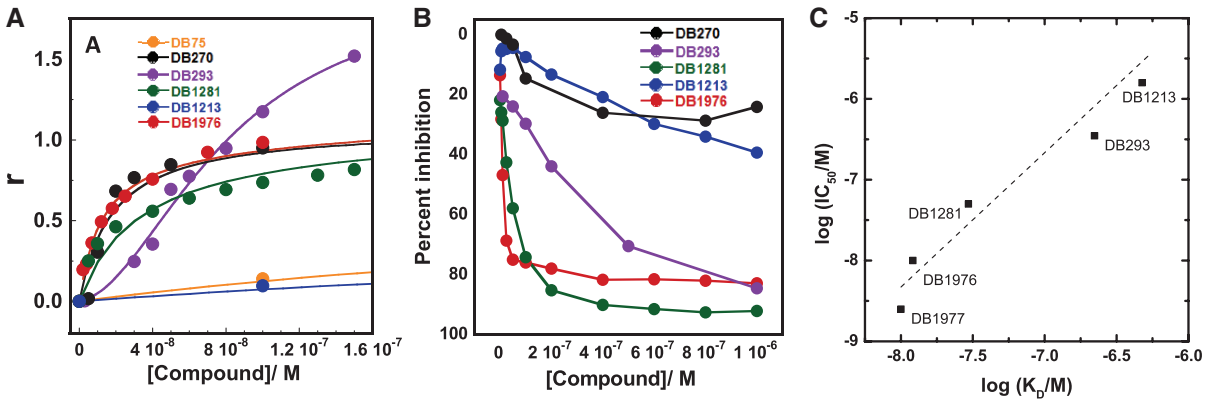

Figure 2. SPR analysis of the dications binding to the λB site and inhibition of PU.1. (**A**) The binding of compounds to an immobilized DNA hairpin duplex harboring the λB site was determined by SPR. The *r* values (as explained in the Supplementary Methods) are plotted against compound concentration. An appropriate one or two site (DB293) model was used to fit the data. Additional points at higher concentration were used to obtain the K_D values for DB75 and DB1213. DB1977 is similar to DB1976 and is not shown. Numerical estimates of K_D are given in Table 1. (**B**) The protein inhibition signal in percentage is plotted against compound concentration. Numerical estimates of IC_{50} are given in Table 1. (**C**) Comparison of DNA-binding affinity and PU.1-inhibitory potency of DB compounds. For DB293, the K_D value for binding the first equivalent of drug is used.

Table 1. Binding affinities and PU.1-inhibitory potencies of heterocyclic diamidines

	Direct binding SPR	PU.1 inhibition			
		SPR	EMSA		Live cells
Compound	log K_D[a]	log IC_{50}	log IC_{50}[b]	$-n_H$[b]	log IC_{50}[b]
DB1977	−8.00	−8.60	−8.51 ± 0.11	1.5 ± 0.30	−6.24 ± 0.03
DB1976	−7.92	−8.00	−8.09 ± 0.07	0.86 ± 0.13	−5.42 ± 0.04
DB1281	−7.53	−7.30	−7.79 ± 0.05	1.4 ± 0.2	>−4
DB293	−6.65, −7.42	−6.46	−6.47 ± 0.03	2.3 ± 0.3	
DB270	−7.74	—[c]			
DB1213	−6.32	∼−5.8			
DB75	−6.27	—[c]			

[a]Fitted value from Equation (2) in Supplementary Methods.
[b]Fitted values from Equation (3) in Supplementary Methods.
[c]Insufficient inhibition to estimate IC_{50}.

as the monobenzimidazole-selenophene DB1281. Conversion of the furan in DB270 to a selenophene (DB1976) again produced a significant jump in binding affinity. λB-bound selenophene dications show strong, positive-induced circular dichroism spectra between 350–400 nm (Supplementary Figure SD2), indicative of similar minor-groove recognition as previously established for the furan analogs (37,38). In summary, these compounds bind strongly in the DNA minor groove with structure-dependent variations in binding affinity.

Heterocyclic diamidines inhibit PU.1 binding at the λB site

We have previously optimized SPR for characterizing PU.1–DNA interactions and displacement of PU.1 by the minor-groove binder distamycin (27). With λB sites immobilized in a DNA hairpin duplex a 100 nM solution of the PU.1 ETS domain was injected over the surface with increasing compound concentrations. The strong protein SPR signal diminished as the protein–DNA complex was titrated with increasing concentrations of compounds (Supplementary Figure SD3). This is a clear demonstration that minor-grove binding diamidines, such as those in Figure 1A, are able to block the ability of the PU.1 protein to bind site specifically in the DNA major groove. Steady-state signals were used to determine IC_{50} values in Figure 2C and Table 1. A summary of IC_{50} versus K_D is shown in Figure 2C.

DB75 does not inhibit PU.1 binding and its selenophene analog, DB1213 is a relatively weak inhibitor, IC_{50}∼1.5 μM. With increasing concentrations of the closely related compound, DB293, which has a single phenyl of DB75 replaced by a benzimidazole, the SPR signal is reduced by the maximum amount by 1 μM concentration (Figure 2B). The residual signal is primarily a result of DB293 binding in the minor groove of DNA and non-specific protein binding (27). The protein inhibition curve of DB293 also has a sigmoidal appearance showing cooperative protein inhibition with a moderate IC_{50} (Table 1). The selenophene analog of DB293, DB1281, binds more strongly (K_D = 30 nM) to the DNA than DB293 and DB1281 binding results in strong PU.1-DNA inhibition (IC_{50} = 50 nM). The bisbenzimidazole furan analog of DB293, DB270, binds better than DB293 but, surprisingly, inhibits the PU.1-DNA complex weakly. DB1976, the selenophene analog of DB270, however, potently inhibits PU.1 binding (IC_{50} = 10 nM), in good agreement with the high DB1976-λB affinity (K_D = 12 nM). DB1977 with an imidazoline modification at the amidines gives similar binding constants and IC_{50} values to DB1976.

To test the SPR data, we used the electrophoretic mobility shift assay (EMSA) to assess the inhibition of PU.1 binding by DB293, DB1281, DB1976 and DB1977 (Supplementary Figure SD4 and Table 1). Overall, the results are in agreement with the SPR measurements, but they also reveal additional compound-specific

features in PU.1 inhibition. Specifically, comparison of the DB293/DB1281 pair shows that DB293 (the parent furan) inhibits PU.1 with a Hill coefficient (n_H) of 2.3 ± 0.3, in agreement with the SPR data (Figure 2B). Interestingly, the selenophene displaces PU.1 with greater apparent potency but less cooperatively, albeit with a Hill coefficient still well over unity, highlighting the lack of any coupling between positively cooperative binding and high affinity/inhibitory potency.

In the case of DB1976/DB1977 pair, which differs in terms of their terminal dications, both compounds inhibit PU.1 ETS binding with similarly low IC_{50} values (Table 1), but the associated Hill coefficient for DB1976 (0.86 ± 0.13) is significantly lower than DB1977 (1.5 ± 0.3). The fractional Hill coefficient for DB1976 suggests that it binds two or more sites in the λB motif or a single site with negative cooperativity (or a combination of both). In our empirical fit of the data to total compound concentration, depletion of high-affinity ligand would overestimate the Hill coefficient (39). The situation with DB1977 is additionally complicated by its poor solubility and tendency to aggregate; it was not possible to maintain DB1977 above ~0.1 μM in Tris buffer. We, therefore, expect the true values of n_H for DB1976 to be <0.86 still and for DB1977, closer to unity. In summary, compound modifications profoundly affect the ability of the dications to inhibit TFs, from no to low nM inhibition.

Structural heterogeneity in compound-λB binding

To understand the compound-specific differences in PU.1 inhibition in greater detail, we performed DNA footprinting to identify where the four compounds, examined by electrophoretic mobility shift, bind in the λB motif. Using DNase I and hydroxyl radical (•OH) as minor-groove probes, we compared the footprints of a DNA fragment harboring the λB motif at saturating concentrations of compounds relative to the unbound state. For the DB293/DB1281 pair (Figure 3), DB1281 protected the λB motif from •OH prominently at both minor grooves (marked S1 and S2) flanking the ETS core consensus (5′-GGAA-3′). In contrast, even at a saturating concentration of 0.1 mM, DB293 appeared to bind only the S1 site (the AT-rich track 5′ to the GGAA consensus), and protected against •OH more weakly than DB1281. We independently verified DB293 binding to S1 and the negligible occupancy at S2 by DNase I footprinting (Supplementary Figure SD1). Remarkably, occupancy at S1 by DB293 induces a distinct hypersensitivity to •OH at positions (asterisks in Figure 3) distal to its binding site at S1,

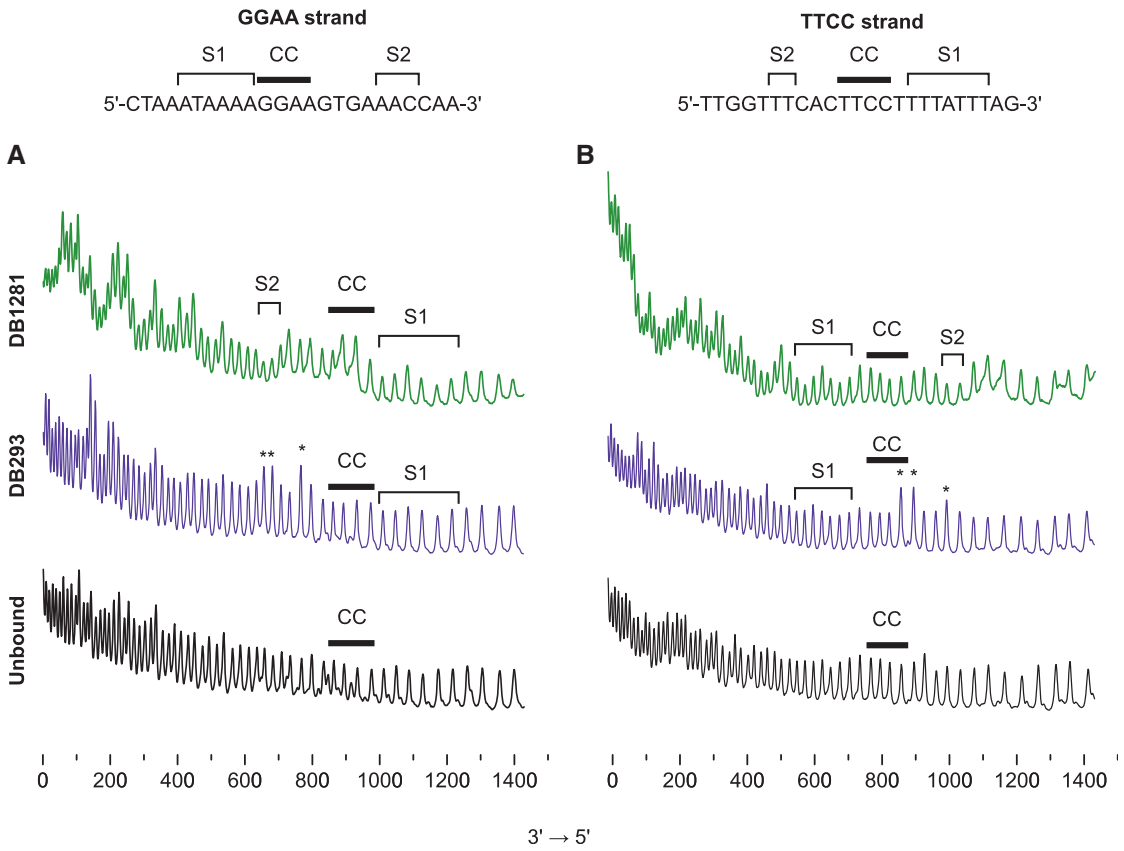

Figure 3. DB293 induces distinct DNA conformations at the λB motif that are not shared by its homolog DB1281. A DNA fragment harboring the λB site was saturated with DB293 (0.1 mM) or DB1281 (1 μM) and probed by hydroxyl radicals (•OH). Shown here are the lane traces for the 5′-GGAA-3′ and 5′-TTCC-3′ strands; the experimental gel images are found in Supplementary Figure SD5. The pixel count is marked in the abscissa. Note the 3′→5′ direction from left to right. Although the two •OH footprints within the λB motif for DB1281 are apparent, neither strand exhibits protection by DB293 at S2. Instead, DB293 induces local hypersensitivity to •OH at both strands just 3′ to the CC. DNase I footprinting confirms the weak footprint at S1 and negligible occupancy at S2 for DB293 (Supplementary Figure SD1).

reaching as far as bases corresponding to S2. Taken together with the SPR and gel shift data, we conclude that DB293 binds as a cooperative dimer ($n_H \sim 2$), albeit weakly, at a single flanking site S1 (5′-ATAAAA-3′). The lower apparent Hill coefficient ($n_H \sim 1.4$) for DB1281 then follows as a consequence of a second high-affinity binding site at S2.

In the case of DB1976 and DB1977, DNase I footprinting detects a strong binding site in the AT-rich track (5′-A TAAAA-3′) upstream from the ETS consensus (S1) (Figure 4A and B). The •OH footprinting identifies a second binding site (5′-AAAC-3′ in S2) in the other flanking segment for DB1976 only (Figure 4C and D). These two sites are sufficiently separated to account for the fractional Hill coefficient associated with DB1976. Evidence that the two sites interact may be found in the DNase I footprints, in which bases between S1 and S2 (hollow square and hollow circle in Figure 4A and B) are also protected by DB1976 but not DB1977. In summary, the underlying effects of compound binding and induced changes in DNA structure are significant and variable from one compound to the next.

The heterocyclic dications inhibit PU.1-dependent transactivation differentially in live cells

To probe the potential of compounds to inhibit gene activation by PU.1 *in vivo*, we developed a specific cell-based reporter assay for PU.1. We cloned a reporter plasmid, pλB×5-EGFP, in which a series of 5× tandem λB motifs were placed just upstream from a minimal TATA-promoter to drive the expression of an EGFP reporter. Specificity for PU.1 is conferred by using a cell line, HEK293, which does not natively express PU.1. Thus, transfection of pλB×5-EGFP in HEK293 generated no signal beyond the autofluorescence of untransfected cells (Figure 5A). Prior transfection with an expression plasmid for PU.1 24 h before transfecting pλB×5-EGFP readily activated the reporter. Without binding sites for additional TFs, the transactivation efficiency of pλB×5-EGFP is relatively low (∼10%). To ensure reliable counting statistics by flow cytometry, we have gated and statistically powered our measurements (>20 000 counts/sample) to detect a 2% event frequency with a CV of <5%.

We tested the inhibition of EGFP fluorescence from pλB×5-EGFP by titrating the three compounds in our series that demonstrate the lowest IC_{50}: DB1976, DB1977 and DB1281. Although DB1976 and DB1977 inhibit cellular EGFP fluorescence with an IC_{50} ∼3 μM and 0.5 μM (Table 1), respectively, DB1281 exerts no apparent effect up to an extracellular concentration of 100 μM (Figure 5B). To probe whether the loss of cellular EGFP fluorescence may be due to compound-induced cytotoxicity, we assayed the metabolic status of HEK293 cells by resazurin reduction at the same compound concentrations. None of the three compounds were toxic to HEK293 cells at concentrations up to 10 μM, demonstrating the inhibition of EGFP signal was not due to indirect effects related to cytotoxicity (Figure 5B). In summary, DB1976 and DB1977 inhibit PU.1-specific gene transactivation in live cells, and do so without toxicity.

Localization of compounds in live unfixed cells

To further understand the biological basis of these unexpected differences in PU.1 inhibition among the compounds, we evaluated the cellular uptake of the compounds by fluorescence microscopy. The compounds absorb between 350–400 nm (c.f. Supplementary Figure SD2) and emit a blue fluorescence. HEK293 cells were incubated with 10 μM compounds for 24 h and then counterstained with 2 μg/ml DOX for 30 min. DOX fluoresces at a non-overlapping wavelength (red) and rapidly concentrates in live (unfixed) cell nuclei without short-term toxicity (40,41). Nuclear uptake of the heterocyclic cations was visualized and measured in terms of colocalization with DOX. All three compounds codistribute extensively with DOX, indicative of nuclear selectivity (Figure 6A). Quantitative analysis, however, reveal differences among the three compounds (Figure 6B). On one hand, the fluorescence of DB1976 not only quantitatively co-occurs with DOX but also correlates strongly in signal intensity ($r = 0.90$). On the other hand, a significant fraction of DB1281 fluorescence (16%) did not colocalize with DOX, and the colocalized fluorescence intensities of DB1281 and DOX are less correlated ($r = 0.58$; arrows in Figure 6A). DB1977 exhibits intermediate colocalization and correlation with DOX. In summary, DB1976 is largely localized similarly to DOX in the nucleus, whereas DB1281 and, to a lesser extent, DB1977, associate with cellular components outside the nucleus, and heterogeneously within the nucleus.

DISCUSSION

Our expanding knowledge of genes, their regulatory sequences, as well as the TFs and enzymes which regulate their expression provides attractive targets for external control by designed small molecules. Design of small molecules to target TFs, however, has not been highly successful. The TFs lack the substrate and inhibitor binding sites normally present in enzymes and this makes small molecule design to specifically target them difficult. A natural approach is to target TFs is to modulate their binding to DNA. The development of DNA-binding polyamides has produced some promising results (7–11). Aryl diamidines and related compounds have a long history of use as pharmaceuticals and as nuclear stains in cells. For these reasons we are pursuing these compounds as potential TF inhibitors. We report here a new series of heterocyclic diamidines or di-imidazolines that include potent inhibitors of the ETS TF PU.1 at the protein–DNA level. All ETS proteins recognize 10-bp sites harboring a central 5′-GGAA/T-3′ core consensus and variable flanking sequences. The flanking sequences are non-random and genomic studies have established clear sequence preferences for high-affinity binding by subsets of ETS members *in vivo* (42). PU.1 belongs to a small class of ETS proteins (class III) that are strongly selective for

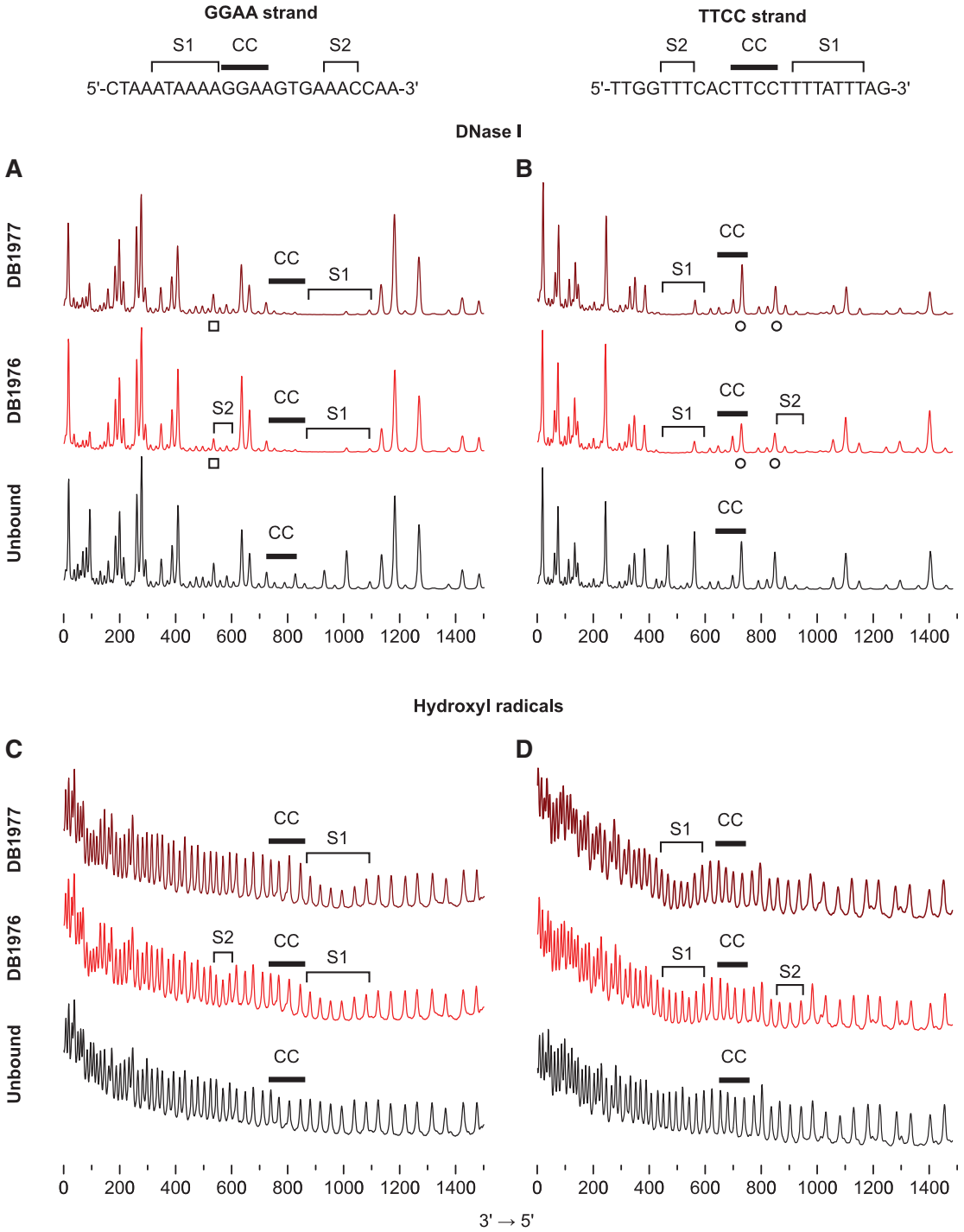

Figure 4. The homologs DB1976 and DB1977 differentially recognize AT-rich sequences within the λB motif, a PU.1-specific binding site. A DNA fragment harboring the λB site was saturated with DB1976 (1 μM) or DB1977 (0.1 μM) and probed by DNase I (**A** and **B**) or hydroxyl radicals (•OH; **C** and **D**). Shown here are the lane traces for the 5′-GGAA-3′ and 5′-TTCC-3′ strands; the experimental gel images are found in Supplementary Figure SD6. The pixel count is marked in the abscissa. Note the 3′ → 5′ direction from left to right. Bases marked by hollow symbols (square, circle) are significantly more protected against DNase I by DB1976 than DB1977. DNase I protection by DB1976 may, therefore, be considered as a single, extended footprint. Whereas the two •OH footprints for DB1976 are apparent (S1 ad S2), neither strand exhibits protection by DB1977 at S2.

AT-rich flanking sequences, a feature distinct from other ETS classes (30,43). Together with potential applications of PU.1 inhibition in several autoimmune disorders, our data represent a significant advance in transcriptional control of ETS TFs.

Structure-function relationships in λB-binding and PU.1 inhibition by compounds

As the compounds bind in the DNA minor groove, they must inhibit PU.1 binding by an allosteric mechanism.

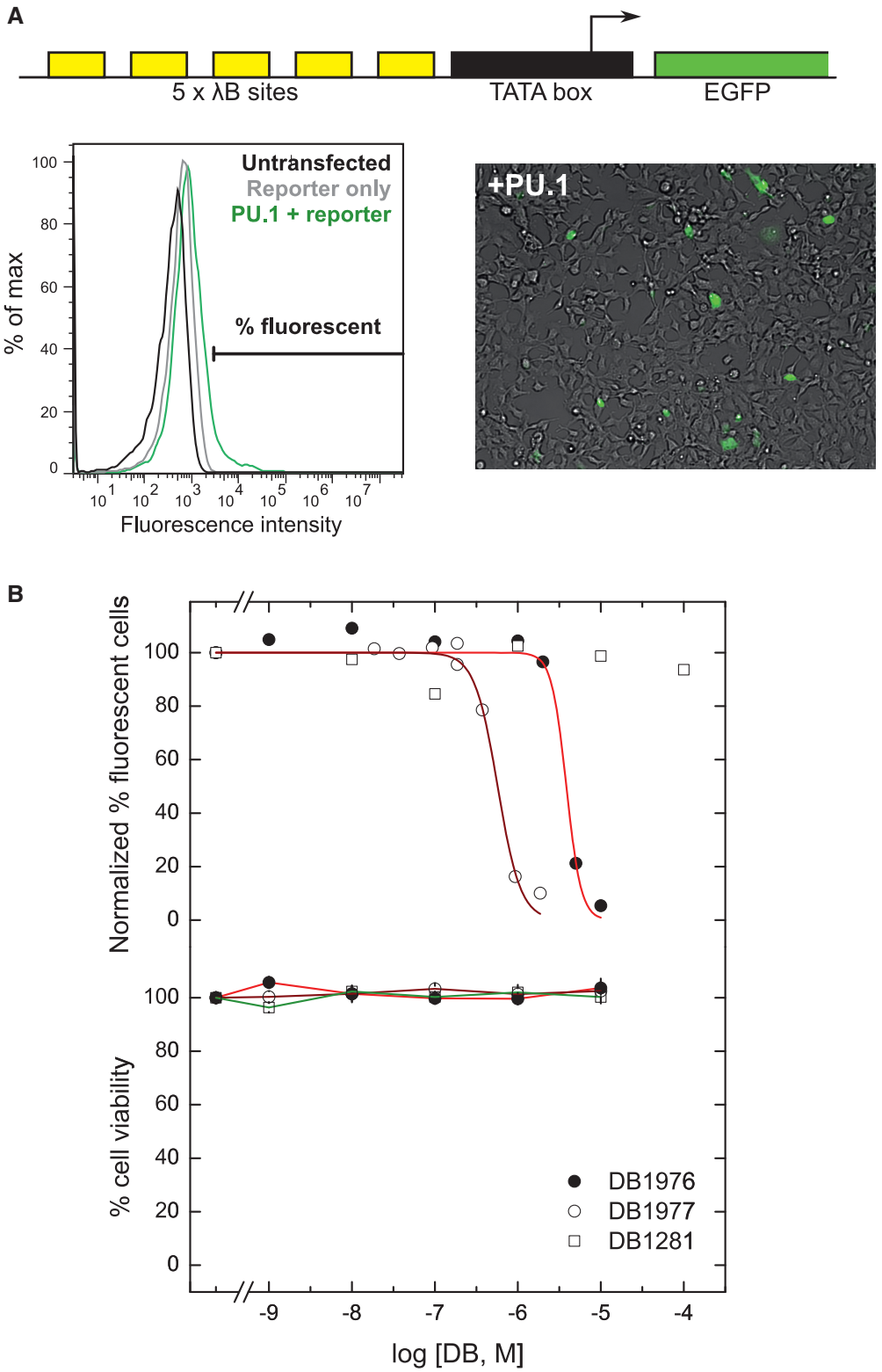

Figure 5. Inhibition of PU.1-specific gene transactivation in live cells. (**A**) PU.1 activity was assayed using an EGFP reporter under the control of a minimal TATA-box promoter. An enhancer element consisting of five tandem λB sites, spaced one helical turn apart, confers specificity to PU.1. Reporter expression was measured by flow cytometry. The HEK293 cells, which do not express PU.1, do not activate the reporter except in the presence of exogenous PU.1 (as shown in fluorescence micrograph). (**B**) PU.1-expressing HEK293 cells were transfected with reporter plasmid with or without DB1976, DB1977 or DB1281 in the culture medium at the indicated concentrations. EGFP fluorescence was measured by flow cytometry after 24 h. The effect of the compounds on cell viability was separately determined by resazurin reduction.

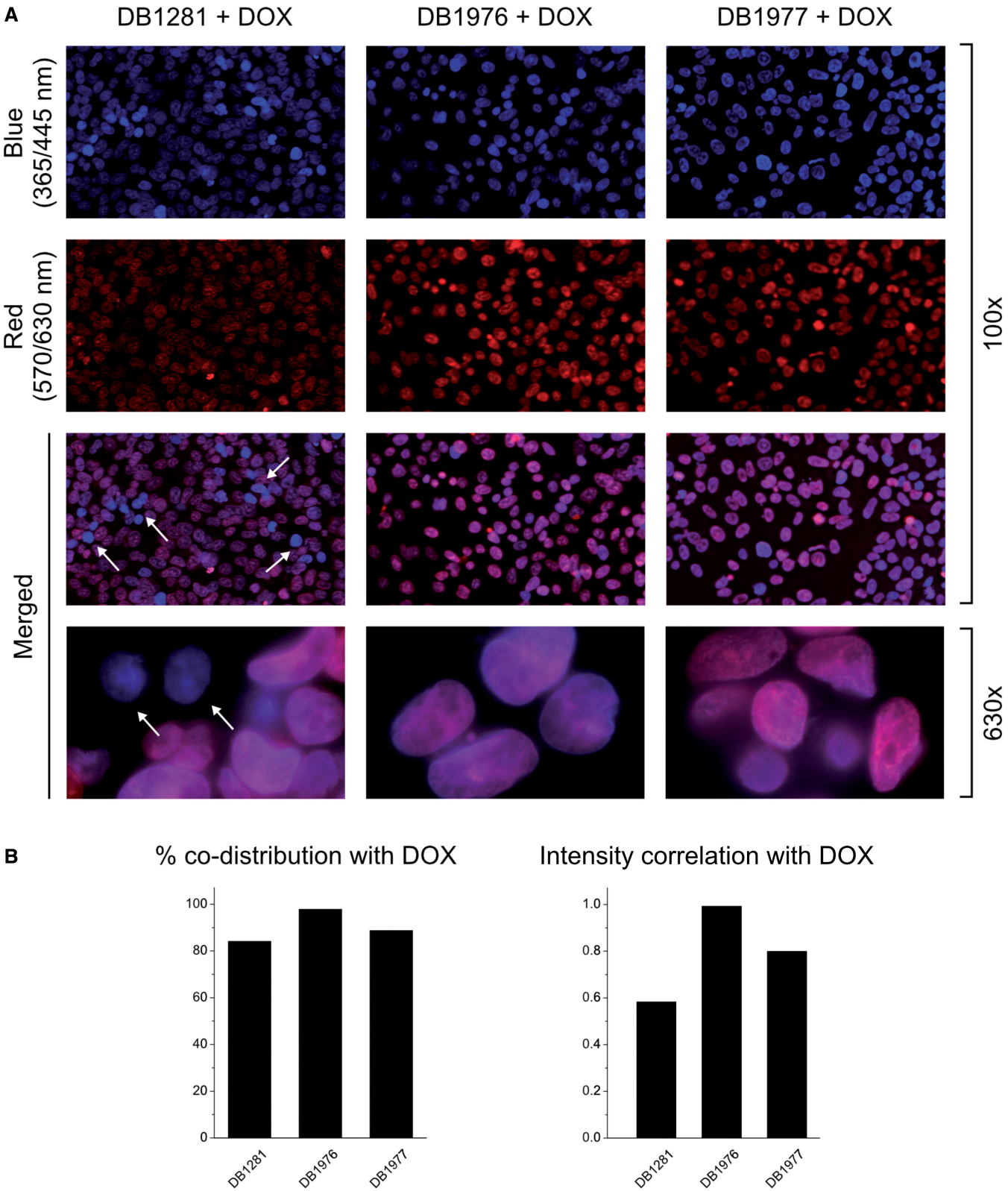

Figure 6. Localization of DB compounds in live unfixed HEK293 cells. (**A**) The uptake of DB1281, DB1976, and DB1977 by HEK293 cells and colocalization with DOX were monitored by fluorescence microscopy as described in 'Materials and Methods'. Arrows indicate cells that show particularly strong DOX staining in DB1281. (**B**) Quantitative colocalization analysis of the dications and DOX fluorescence in terms of spatial co-distribution and intensity correlation. DB1281 correlates comparably as DB1976 and DB1977 in terms of spatial codistribution with DOX but not DOX intensity.

Our goal in this work was to find compounds that are most effective at this type of inhibition. Single modifications of furamidine, DB75, resulted in minor gains in affinity for the λB site. Such was the case whether the modification was a furan → selenophene (DB1213) or phenyl → monobenzimidazole (DB293) substitution. However, the combined modifications in DB1281 improved affinity by ∼10 fold. These observations are reminiscent of the related thiophene derivative, DB818, which binds better than DB293 to the minor groove in AT sequences due to a better optimized shape for minor-groove recognition (44). In the case of DB1281, however, the footprinting data implicate a second high-affinity site downstream from the 5′-GGAA-3′ ETS consensus as an additional reason for the enhanced affinity.

In a similar way, replacement of the second phenyl by benzimidazole in DB270 improved affinity similarly as DB1281. The extra surface area of the additional benzimidazole for interaction with the walls of the minor groove and the extra H-bonding benzimidazole-NH are responsible for this improvement. Surprisingly, DB270 is a poor competitor for PU.1 binding, and additional studies are underway to determine the cause of its lack of inhibition. Importantly DB1976, the selenophene analog of DB270, potently inhibits PU.1. Thus, the inhibition disadvantage in DB270 is effectively relieved by the larger C-Se-C bond angle in DB1976 (38). It seems likely that the Se derivative is a much better allosteric effector for PU.1 inhibition.

Heterogeneity in compound-λB interactions

The SPR and gel mobility shift titrations as well as DNA footprinting data reveal structural and conformational heterogeneity that attends the sequence-selective binding of the dications. We observed heterogeneity in terms of the number of binding sites along the λB motif and conformation of the compounds bound to DNA. In addition to the AT-rich binding site (S1) just upstream from the 5′-GGAA-3′ ETS consensus, DB1281 and DB1976 also bind at a second AT-rich site (S2) downstream from the consensus. In the case of DB1281, its greater potency in PU.1 inhibition relative to DB293 may, at least in part, be attributed to the availability of S2 as occupancy by the drug at either site would displace the protein. However, the presence of a second binding site for DB1976 has a much more marginal effect on PU.1 inhibition and direct binding affinity. These comparisons indicate that neither the location nor number of binding sites alone dictates the overall behavior of a compound in terms of binding affinity or inhibitory potency and imply complex site–site interactions for compounds such as DB1976.

As direct interactions between compounds in the DNA-bound state may be discounted, the notion of site–site interactions requires conformational changes in the intervening DNA to communicate the occupancy at each site. The footprinting data show that induced DNA conformation occurs and represents another important determinant of the thermodynamics of compound binding. Allosteric effects of the bound molecules on the protein–DNA interactions at both flanking sequences of the GGAA consensus could, therefore, synergistically modulate PU.1 binding more than either alone. The binding of DB293 to a specific flanking site (S1) upstream from the ETS consensus, for example, induces conformation changes in the 3′ direction that are detectable as minor-groove hypersensitivity to hydroxyl radicals (•OH). Similarly, the occupancy of DB1976 at sites flanking both sides of the ETS consensus induces conformational changes in the intervening sequence, but in the case detectable as minor-groove *protection* against DNase I. Therefore, these conformational changes are specific to each compound, indicating the ability of even short sequences to discriminate among them. In particular, the specificity of compound-induced conformational changes further implies that, although they all bind to the S1 site, the details of their interactions with DNA contacts in the minor groove are likely different. Our data highlight the utility of DNase I and •OH footprinting as complementary probes that are sensitive to local structural microheterogeneity. In summary, locally compound-induced DNA structural changes, even of different types, are successful in producing effective allosteric inhibitors of PU.1. The structure and compound property space for the compounds in Figure 1A produces a surprising range of effects on DNA and especially, on inhibition of PU.1 binding.

Inhibition of PU.1 in live cells

To demonstrate the feasibility of inhibiting PU.1 with heterocyclic diamidines *in vivo*, we used a reporter-based assay designed to respond to transactivation by PU.1. The data show that DB1976 and DB1977 inhibited PU.1 activity with IC_{50} in the sub- to low-micromolar range. These values, which are 10^2-fold higher than those observed in SPR or gel shift experiments (Table 1), are expected owing to the protected nature of DNA in the nucleus. Significantly, DB1281, which strongly inhibits specific PU.1 binding *in vitro*, shows no detectable activity in live cells. As none of the compounds tested exhibit detectable cytotoxicity (Figure 5B), more subtle biological factors are at play. Although all three compounds codistribute extensively in the nucleus, significant quantitative differences exist among them (Figure 6). DB1281, in particular, exhibits significant distribution outside the nucleus (not colocalized with DOX) as well as a peculiar distribution within the nucleus (low correlation with colocalized DOX). Thus, a substantial fraction of intracellular and even intranuclear DB1281 may be sequestered, and therefore unavailable for binding to its target sites. This is a critical feature of compound biological activity that is often overlooked. We note that our use of DOX as a nuclear counterstain was aimed at preserving the biological disposition of the test compounds by avoiding potential artifacts of fixation (required, for example, with the use of propidium) on DNA binding ligands (45). The lack of toxicity and perturbation on cellular function due to short-term (30 min.) exposure to DOX is also well-established (40,41). Thus, we consider our results to be biologically reliable.

For applications outside of cancer chemotherapy or immunosuppression, correction of aberrant gene expression

without adversely affecting cell viability is highly desirable. The ability of DB1976 and DB1977 to abolish PU.1-dependent gene transactivation without detectable toxicity is, therefore, a significant feature. This is in contrast to the reported cytotoxicity of some dications at 10^{-6} M concentrations in cultured cancer cell lines (46). This difference may possibly be related to our use of a non-malignant cell line (HEK293). Given the potential of PU.1 inhibition in non-cancer indications, the lack of apparent cytotoxicity is a welcome and encouraging result of our study. The low toxicity also suggests that these type compounds can be developed for humans, and the extensive clinical experience with diamidines in the treatment of trypanosomiasis and other diseases (47) is a significant advantage over other classes of DNA-targeting agents. In conclusion, the effective cellular inhibition of the PU.1 TF observed here with a new series of heterocyclic dications shows that this class of compounds has promise for development as therapeutics for specific inhibition of TF–DNA complexes. The variety of effects and exciting inhibition results produced by the set of compounds in our study highlights the need to conduct a wider range of experiments in our efforts to understand, design and develop DNA-targeted TF inhibitors.

SUPPLEMENTARY DATA

Supplementary Data are available at NAR Online, including [37,38,48,49].

FUNDING

National Institutes of Health [AI064200 to W.D.W. and D.W.B.]; College of Pharmacy, Washington State University (to G.M.K.P.). Funding for open access charge: College of Pharmacy, Department of Pharmaceutical Sciences, Washington State University.

Conflict of interest statement. None declared.

REFERENCES

1. Levine,M. and Tjian,R. (2003) Transcription regulation and animal diversity. *Nature*, **424**, 147–151.
2. Babu,M.M., Luscombe,N.M., Aravind,L., Gerstein,M. and Teichmann,S.A. (2004) Structure and evolution of transcriptional regulatory networks. *Curr. Opin. Struct. Biol.*, **14**, 283–291.
3. Darnell,J.E. Jr. (2002) Transcription factors as targets for cancer therapy. *Nat. Rev. Cancer*, **2**, 740–749.
4. Koehler,A.N. (2010) A complex task? Direct modulation of transcription factors with small molecules. *Curr. Opin. Chem. Biol.*, **14**, 331–340.
5. Okamoto,T., Zobel,K., Fedorova,A., Quan,C., Yang,H., Fairbrother,W.J., Huang,D.C.S., Smith,B.J., Deshayes,K. and Czabotar,P.E. (2012) Stabilizing the pro-apoptotic BimBH3 Helix (BimSAHB) does not necessarily enhance affinity or biological activity. *ACS Chem. Biol.*, **8**, 297–302.
6. Shim,M.S. and Kwon,Y.J. (2010) Efficient and targeted delivery of siRNA *in vivo*. *FEBS J.*, **277**, 4814–4827.
7. Chenoweth,D.M., Harki,D.A., Phillips,J.W., Dose,C. and Dervan,P.B. (2009) Cyclic pyrrole-imidazole polyamides targeted to the androgen response element. *J. Am. Chem. Soc.*, **131**, 7182–7188.
8. Dickinson,L.A., Trauger,J.W., Baird,E.E., Dervan,P.B., Graves,B.J. and Gottesfeld,J.M. (1999) Inhibition of Ets-1 DNA binding and ternary complex formation between Ets-1, NF-kappaB, and DNA by a designed DNA-binding ligand. *J. Biol. Chem.*, **274**, 12765–12773.
9. Moretti,R., Donato,L.J., Brezinski,M.L., Stafford,R.L., Hoff,H., Thorson,J.S., Dervan,P.B. and Ansari,A.Z. (2008) Targeted chemical wedges reveal the role of allosteric DNA modulation in protein-DNA assembly. *ACS Chem. Biol.*, **3**, 220–229.
10. Zhang,Y., Sicot,G., Cui,X., Vogel,M., Wuertzer,C.A., Lezon-Geyda,K., Wheeler,J., Harki,D.A., Muzikar,K.A., Stolper,D.A. *et al.* (2011) Targeting a DNA binding motif of the EVI1 protein by a pyrrole-imidazole polyamide. *Biochemistry*, **50**, 10431–10441.
11. Chiang,S.-Y., Burli,R.W., Benz,C.C., Gawron,L., Scott,G.K., Dervan,P.B. and Beerman,T.A. (2000) Targeting the Ets binding site of the HER2/neu promoter with pyrrole-imidazole polyamides. *J. Biol. Chem.*, **275**, 24246–24254.
12. Peixoto,P., Liu,Y., Depauw,S., Hildebrand,M.-P., Boykin,D.W., Bailly,C., Wilson,W.D. and David-Cordonnier,M.-H. (2008) Direct inhibition of the DNA-binding activity of POU transcription factors Pit-1 and Brn-3 by selective binding of a phenyl-furan-benzimidazole dication. *Nucleic Acids Res.*, **36**, 3341–3353.
13. Nhili,R., Peixoto,P., Depauw,S., Flajollet,S., Dezitter,X., Munde,M.M., Ismail,M.A., Kumar,A., Farahat,A.A., Stephens,C.E. *et al.* (2013) Targeting the DNA-binding activity of the human ERG transcription factor using new heterocyclic dithiophene diamidines. *Nucleic Acids Res.*, **41**, 125–138.
14. Hollenhorst,P.C., McIntosh,L.P. and Graves,B.J. (2011) Genomic and biochemical insights into the specificity of ETS transcription factors. *Annu. Rev. Biochem.*, **80**, 437–471.
15. Oikawa,T. and Yamada,T. (2003) Molecular biology of the Ets family of transcription factors. *Gene*, **303**, 11–34.
16. Sharrocks,A.D. (2001) The ETS-domain transcription factor family. *Nat. Rev. Mol. Cell Biol.*, **2**, 827–837.
17. Sementchenko,V.I. and Watson,D.K. (2000) Ets target genes: past, present and future. *Oncogene*, **19**, 6533–6548.
18. Hsu,T., Trojanowska,M. and Watson,D.K. (2004) Ets proteins in biological control and cancer. *J. Cell. Biochem.*, **91**, 896–903.
19. Gilliland,D.G. (2001) The diverse role of the ETS family of transcription factors in cancer. *Clin. Cancer Res.*, **7**, 451–453.
20. Oikawa,T. (2004) ETS transcription factors: possible targets for cancer therapy. *Cancer Sci.*, **95**, 626–633.
21. Galang,C.K., Muller,W.J., Foos,G., Oshima,R.G. and Hauser,C.A. (2004) Changes in the expression of many Ets family transcription factors and of potential target genes in normal mammary tissue and tumors. *J. Biol. Chem.*, **279**, 11281–11292.
22. Ghanim,H., Mohanty,P., Deopurkar,R., Ling Sia,C., Korzeniewski,K., Abuaysheh,S., Chaudhuri,A. and Dandona,P. (2008) Acute modulation of toll-like receptors by insulin. *Diabetes Care*, **31**, 1827–1831.
23. Gregory,S.G., Schmidt,S., Seth,P., Oksenberg,J.R., Hart,J., Prokop,A., Caillier,S.J., Ban,M., Goris,A., Barcellos,L.F. *et al.* (2007) Interleukin 7 receptor [alpha] chain (IL7R) shows allelic and functional association with multiple sclerosis. *Nat. Genet.*, **39**, 1083–1091.
24. DeKoter,R.P., Lee,H.-J. and Singh,H. (2002) PU.1 regulates expression of the interleukin-7 receptor in lymphoid progenitors. *Immunity*, **16**, 297–309.
25. Penaranda,C., Kuswanto,W., Hofmann,J., Kenefeck,R., Narendran,P., Walker,L.S., Bluestone,J.A., Abbas,A.K. and Dooms,H. (2012) IL-7 receptor blockade reverses autoimmune diabetes by promoting inhibition of effector/memory T cells. *Proc. Natl Acad. Sci. USA*, **109**, 12668–12673.
26. Ohbo,K., Takasawa,N., Ishii,N., Tanaka,N., Nakamura,M. and Sugamura,K. (1995) Functional analysis of the human interleukin 2 receptor γ chain gene promoter. *J. Biol. Chem.*, **270**, 7479–7486.
27. Munde,M., Poon,G.M.K. and Wilson,W.D. (2013) Probing the electrostatics and pharmacological modulation of sequence-specific binding by the DNA-binding domain of the ETS family transcription factor PU.1: a binding affinity and kinetics investigation. *J. Mol. Biol.*, **425**, 1655–1669.
28. Poon,G.M.K. (2012) Sequence discrimination by DNA-binding domain of ETS family transcription factor PU.1 is linked to specific hydration of protein-DNA interface. *J. Biol. Chem.*, **287**, 18297–18307.

29. Poon,G.M.K. (2012) DNA binding regulates the self-association of the ETS domain of PU.1 in a sequence-dependent manner. *Biochemistry*, **51**, 4096–4107.
30. Szymczyna,B.R. and Arrowsmith,C.H. (2000) DNA binding specificity studies of four ETS proteins support an indirect read-out mechanism of protein-DNA recognition. *J. Biol. Chem.*, **275**, 28363–28370.
31. Chenoweth,D.M. and Dervan,P.B. (2009) Allosteric modulation of DNA by small molecules. *Proc. Natl Acad. Sci. USA*, **106**, 13175–13179.
32. Eisenbeis,C.F., Singh,H. and Storb,U. (1993) PU.1 is a component of a multiprotein complex which binds an essential site in the murine immunoglobulin lambda 2-4 enhancer. *Mol. Cell. Biol.*, **13**, 6452–6461.
33. Gossen,M. and Bujard,H. (1992) Tight control of gene expression in mammalian cells by tetracycline-responsive promoters. *Proc. Natl Acad. Sci. USA*, **89**, 5547–5551.
34. Costes,S.V., Daelemans,D., Cho,E.H., Dobbin,Z., Pavlakis,G. and Lockett,S. (2004) Automatic and quantitative measurement of protein-protein colocalization in live cells. *Biophys. J.*, **86**, 3993–4003.
35. Dunn,K.W., Kamocka,M.M. and McDonald,J.H. (2011) A practical guide to evaluating colocalization in biological microscopy. *Am. J. Physiol. Cell Physiol.*, **300**, C723–C742.
36. Wang,L., Bailly,C., Kumar,A., Ding,D., Bajic,M., Boykin,D.W. and Wilson,W.D. (2000) Specific molecular recognition of mixed nucleic acid sequences: an aromatic dication that binds in the DNA minor groove as a dimer. *Proc. Natl Acad. Sci. USA*, **97**, 12–16.
37. Wang,L., Carrasco,C., Kumar,A., Stephens,C.E., Bailly,C., Boykin,D.W. and Wilson,W.D. (2001) Evaluation of the influence of compound structure on stacked-dimer formation in the DNA minor groove. *Biochemistry*, **40**, 2511–2521.
38. Liu,Y., Collar,C.J., Kumar,A., Stephens,C.E., Boykin,D.W. and Wilson,W.D. (2008) Heterocyclic diamidine interactions at AT base pairs in the DNA minor groove: effects of heterocycle differences, DNA AT sequence and length. *J. Phys. Chem. B*, **112**, 11809–11818.
39. Wells,J.W. (1992) In: Hulme,E.C. (ed.), *Receptor-Ligand Interactions: a Practical Approach*. IRL Press, Oxford University Press, Oxford [England], New York, pp. 289–395.
40. Ho,W.C., Dickson,K.M. and Barker,P.A. (2005) Nuclear factor-κB induced by doxorubicin is deficient in phosphorylation and acetylation and represses nuclear factor-κB–dependent transcription in cancer cells. *Cancer Res.*, **65**, 4273–4281.
41. Wang,S., Konorev,E.A., Kotamraju,S., Joseph,J., Kalivendi,S. and Kalyanaraman,B. (2004) Doxorubicin induces apoptosis in normal and tumor cells via distinctly different mechanisms: intermediacy Of H2O2- and p53-dependent pathways. *J. Biol. Chem.*, **279**, 25535–25543.
42. Wei,G.H., Badis,G., Berger,M.F., Kivioja,T., Palin,K., Enge,M., Bonke,M., Jolma,A., Varjosalo,M., Gehrke,A.R. *et al.* (2010) Genome-wide analysis of ETS-family DNA-binding *in vitro* and *in vivo*. *EMBO J.*, **29**, 2147–2160.
43. Pham,T.H., Minderjahn,J., Schmidl,C., Hoffmeister,H., Schmidhofer,S., Chen,W., Langst,G., Benner,C. and Rehli,M. (2013) Mechanisms of *in vivo* binding site selection of the hematopoietic master transcription factor PU.1. *Nucleic Acids Res.*, **41**, 6391–6402.
44. Mallena,S., Lee,M.P., Bailly,C., Neidle,S., Kumar,A., Boykin,D.W. and Wilson,W.D. (2004) Thiophene-based diamidine forms a "super" AT binding minor groove agent. *J. Am. Chem. Soc.*, **126**, 13659–13669.
45. Belitsky,J.M., Leslie,S.J., Arora,P.S., Beerman,T.A. and Dervan,P.B. (2002) Cellular uptake of N-methylpyrrole/N-methylimidazole polyamide-dye conjugates. *Bioorgan. Med. Chem.*, **10**, 3313–3318.
46. Lansiaux,A., Tanious,F., Mishal,Z., Dassonneville,L., Kumar,A., Stephens,C.E., Hu,Q., Wilson,W.D., Boykin,D.W. and Bailly,C. (2002) Distribution of furamidine analogues in tumor cells: targeting of the nucleus or mitochondria depending on the amidine substitution. *Cancer Res.*, **62**, 7219–7229.
47. Paine,M.F., Wang,M.Z., Generaux,C.N., Boykin,D.W., Wilson,W.D., De Koning,H.P., Olson,C.A., Pohlig,G., Burri,C., Brun,R. *et al.* (2010) Diamidines for human African trypanosomiasis. *Curr. Opin. Investig. Drugs*, **11**, 876–883.
48. Nanjunda,R., Munde,M., Liu,Y. and Wilson,W.D. (2011) *Real-time Monitoring of Nucleic Acid Interactions with Biosensor Plasmon Resonance in the Book, Methods for Studying DNA/Drug Interactions*. CRC, p. 392. Taylor and Francis, Boca Raton, Florida.
49. Rodger,A. and Nordén,B. (1997) *Circular Dichroism and Linear Dichroism*. Oxford University Press, New York.